

Triangle singularities in light axial vector meson decays

Meng-Chuan Du

Institute of High Energy Physics, Chinese Academy of Sciences

In collaboration with Prof. Qiang Zhao

The 7th Aisa-Pacific Conference on Few-Body Problems in Physics,
Guilin, China

2017/08/29

Outline

- Introduction to TSM and light axial vector mesons
- Formalism
- Numerical results
- Conclusions

Introduction

- Experiment data on light axial vector states are not sufficient for us to have a full understanding of these states. (e.g. h_1, f_1)
- Strong coupling to $K^*\bar{K}$ threshold gives the possibility of decay through triangle diagram
- Triangle singularity may cause observable effects in the spectrum of light axial vector states.
- A combined analysis on these states is necessary and can provide a coherent picture for their underlying transition dynamics.

f_1	$0^+1^{++},$ $\rightarrow K\bar{K}\pi, \eta\pi\pi, [3\pi]$	$\frac{1}{\sqrt{2}}(K^*\bar{K} - \bar{K}^*K)$
a_1	$1^-1^{++},$ $\rightarrow K\bar{K}\pi, 3\pi, [\eta\pi\pi]$	$\frac{1}{\sqrt{2}}(K^*\bar{K} - \bar{K}^*K)$
h_1	$0^-1^{+-},$ $\rightarrow \rho\pi, \omega\eta, (\phi\eta), [\omega\pi], [\rho\eta], [\phi\pi]$	$\frac{1}{\sqrt{2}}(K^*\bar{K} + \bar{K}^*K)$
b_1	$1^+1^{+-},$ $\rightarrow \phi\pi, \omega\pi, \rho\eta, [\rho\pi], [\omega\eta]$	$\frac{1}{\sqrt{2}}(K^*\bar{K} + \bar{K}^*K)$

Ref:Feng-Kun Guo, C. Hanhart, etc. Arxiv:1705, 00141v1 (2017)

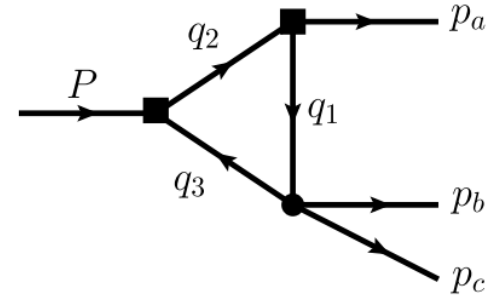


Fig. 1. A typical triangle diagram in which P represents the momentum of light axial vector mesons (e.g. $a_1 f_1 h_1 b_1$), and $q_2 q_3 q_1$ are the momentums of $K^*\bar{K}K$ respectively.

Ref:Jia-Jun Wu, X.H.Liu, Qiang.Zhao, Bing-Song.
Zou, PRL108, 081103(2012);Xiao-Gang Wu, J. J Wu, Qiang. Zhao, Bing-Song.
ZouPRD87, 014023(2013);Xiao-Hai Liu, M. Oka, Qiang Zhao, PLB753, 297(2016);
Also see Feng-Kun Guo' s plenary talk on heavy meson spectroscopy

Observation of $a_1(1420)$

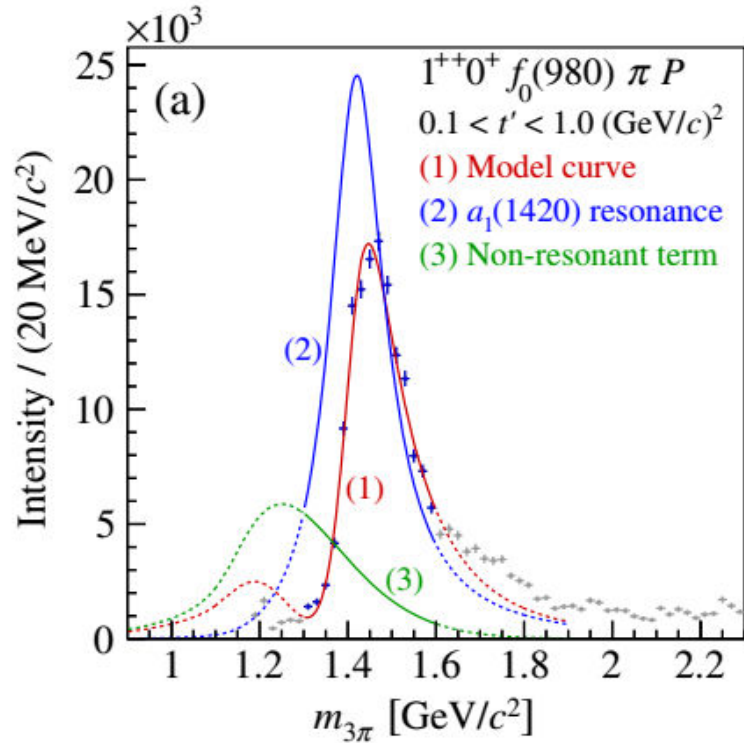


Fig.2 $a_1(1420)$ is observed by COMPASS Collaboration in 2015 in $f_0(980)\pi$ channel.

Ref: C. Adolph, et al. PRL 115, 082001

It was first proposed that the abnormal a_1 state from COMPASS observation could be explained by the kinematics of triangle singularity. See review by Q. Zhao, MENU2016 plenary talk.

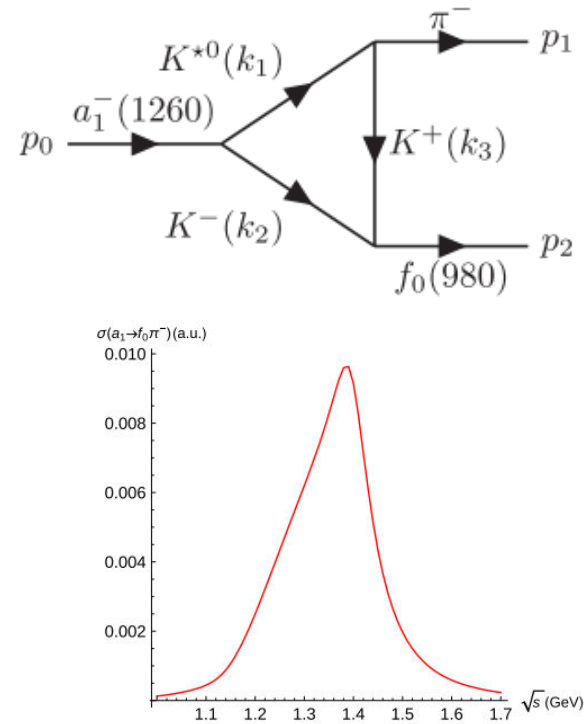
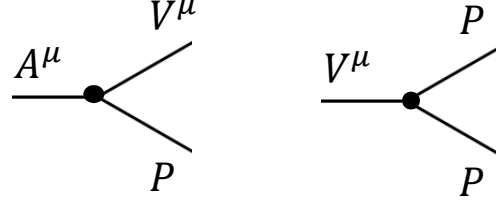


Fig.3 $a_1^- \rightarrow f_0 \pi^-$ P-wave channel due to the rescattering of kaons.

Formalism.



We adopted the following Lagrangians to describe Axial vector-Vector-Pseudovector and Vector-Pseudovector-Pseudovector vertex:

$$L_{A^\pm VP} = g^\pm \text{Tr}[A^{\pm\mu} \cdot [V_\mu, P]^{\mp}] \quad L_{VPP} = g_{VPP} \text{Tr}(V^\mu (\partial_\mu P_1 P_2 - P_1 \partial_\mu P_2))$$

The mixing of h_1 and f_1 are parameterized by:

$$\begin{pmatrix} h_1 \\ h'_1 \end{pmatrix} = \begin{pmatrix} \cos(\theta_{1P_1}) & \sin(\theta_{1P_1}) \\ -\sin(\theta_{1P_1}) & \cos(\theta_{1P_1}) \end{pmatrix} \begin{pmatrix} h_1 \\ h_8 \end{pmatrix} = \begin{pmatrix} \cos(\alpha_{1P_1}) & \sin(\alpha_{1P_1}) \\ -\sin(\alpha_{1P_1}) & \cos(\alpha_{1P_1}) \end{pmatrix} \begin{pmatrix} h_n \\ h_s \end{pmatrix}$$

$$\begin{pmatrix} f_1 \\ f'_1 \end{pmatrix} = \begin{pmatrix} \cos(\theta_{3P_1}) & \sin(\theta_{3P_1}) \\ -\sin(\theta_{3P_1}) & \cos(\theta_{3P_1}) \end{pmatrix} \begin{pmatrix} f_1 \\ f_8 \end{pmatrix} = \begin{pmatrix} \cos(\alpha_{3P_1}) & \sin(\alpha_{3P_1}) \\ -\sin(\alpha_{3P_1}) & \cos(\alpha_{3P_1}) \end{pmatrix} \begin{pmatrix} f_n \\ f_s \end{pmatrix}$$

where $h_1 \equiv h_1(1170)$, $h'_1 \equiv h_1(1380)$, $f_1 \equiv f_1(1285)$, $f'_1 \equiv f_1(1420)$.

h_n and f_n are $\frac{u\bar{u}+d\bar{d}}{\sqrt{2}}$ with different total spin.

$$\alpha = \theta + \arctan\left(\frac{1}{\sqrt{2}}\right)$$

$$A^{-\mu} = \begin{pmatrix} \frac{h_n + b_1^0(1235)}{\sqrt{2}} & b_1^+(1235) & K_{1B}^+ \\ b_1^-(1235) & \frac{h_n - b_1^0(1235)}{\sqrt{2}} & K_{1B}^0 \\ K_{1B}^- & \bar{K}_{1B}^0 & h_s \end{pmatrix}^\mu$$

$$A^{+\mu} = \begin{pmatrix} \frac{f_n + a_1^0(1260)}{\sqrt{2}} & a_1^+(1260) & K_{1A}^+ \\ a_1^-(1260) & \frac{f_n - a_1^0(1260)}{\sqrt{2}} & K_{1A}^0 \\ K_{1A}^- & \bar{K}_{1A}^0 & f_s \end{pmatrix}^\mu$$

$$V_\mu = \begin{pmatrix} \frac{\omega}{\sqrt{2}} + \frac{\rho^0}{\sqrt{2}} & \rho^+ & K^{*+} \\ \rho^- & \frac{\omega}{\sqrt{2}} - \frac{\rho^0}{\sqrt{2}} & K^{*0} \\ K^{*-} & \bar{K}^{*0} & \phi \end{pmatrix}_\mu$$

$$P = \begin{pmatrix} \frac{\eta}{\sqrt{3}} + \frac{\eta'}{\sqrt{6}} + \frac{\pi^0}{\sqrt{2}} & \pi^+ & K^+ \\ \pi^- & \frac{\eta}{\sqrt{3}} + \frac{\eta'}{\sqrt{6}} - \frac{\pi^0}{\sqrt{2}} & K^0 \\ K^- & \bar{K}^0 & -\frac{\eta}{\sqrt{3}} + \sqrt{\frac{2}{3}}\eta' \end{pmatrix}$$

Formalism.

The physical $K_1(1400)$ and $K_1(1270)$ are also mixed objects of K_{1A} and K_{1B} in 1^{++} and 1^{+-} octets respectively with mixing angle θ_{K_1} :

$$\begin{pmatrix} K_{1A} \\ K_{1B} \end{pmatrix} = \begin{pmatrix} \cos(\theta_{K_1}) & -\sin(\theta_{K_1}) \\ \sin(\theta_{K_1}) & \cos(\theta_{K_1}) \end{pmatrix} \begin{pmatrix} K_1(1400) \\ K_1(1270) \end{pmatrix}$$

Therefore their mass are given by:

$$m_{K_{1A}}^2 = m_{K_1(1400)}^2 \cos^2(\theta_{K_1}) + m_{K_1(1270)}^2 \sin^2(\theta_{K_1})$$

$$m_{K_{1B}}^2 = m_{K_1(1400)}^2 \sin^2(\theta_{K_1}) + m_{K_1(1270)}^2 \cos^2(\theta_{K_1})$$

With Gell-Mann-Okubo relation:

$$m_{1P_1}^2 = \frac{4m_{K_{1B}}^2 - m_{b_1}^2}{3}, m_{3P_1}^2 = \frac{4m_{K_{1A}}^2 - m_{a_1}^2}{3}$$

The mixing angle of h_1 and f_1 are connected by

$$\left\{ \begin{array}{l} \tan(\theta_{1P_1}) = \frac{m_{h'_1}^2 - m_{1P_1}^2}{\sqrt{m_{1P_1}^2(m_{h'_1}^2 + m_{h_1}^2 - m_{1P_1}^2) - m_{h_1}^2 m_{h'_1}^2}} \\ \tan(\theta_{3P_1}) = \frac{m_{f'_1}^2 - m_{3P_1}^2}{\sqrt{m_{3P_1}^2(m_{f'_1}^2 + m_{f_1}^2 - m_{3P_1}^2) - m_{f_1}^2 m_{f'_1}^2}} \end{array} \right.$$

So that one can calculate $\theta_{1P_1}(\theta_{3P_1})$ as soon as $\theta_{3P_1}(\theta_{1P_1})$ is given.

(The same goes for α_{1P_1} and α_{3P_1})

$$\begin{pmatrix} h_1 \\ h'_1 \end{pmatrix} = \begin{pmatrix} \cos(\theta_{1P_1}) & \sin(\theta_{1P_1}) \\ -\sin(\theta_{1P_1}) & \cos(\theta_{1P_1}) \end{pmatrix} \begin{pmatrix} h_1 \\ h_8 \end{pmatrix} = \begin{pmatrix} \cos(\alpha_{1P_1}) & \sin(\alpha_{1P_1}) \\ -\sin(\alpha_{1P_1}) & \cos(\alpha_{1P_1}) \end{pmatrix} \begin{pmatrix} h_n \\ h_s \end{pmatrix}$$

$$\begin{pmatrix} f_1 \\ f'_1 \end{pmatrix} = \begin{pmatrix} \cos(\theta_{3P_1}) & \sin(\theta_{3P_1}) \\ -\sin(\theta_{3P_1}) & \cos(\theta_{3P_1}) \end{pmatrix} \begin{pmatrix} f_1 \\ f_8 \end{pmatrix} = \begin{pmatrix} \cos(\alpha_{3P_1}) & \sin(\alpha_{3P_1}) \\ -\sin(\alpha_{3P_1}) & \cos(\alpha_{3P_1}) \end{pmatrix} \begin{pmatrix} f_n \\ f_s \end{pmatrix}$$

Fig. 4. Reminder of the definition of Mixing angle of h_1 and f_1 states in previous page. $\alpha = \theta + \arctan(\frac{1}{\sqrt{2}})$

Production:

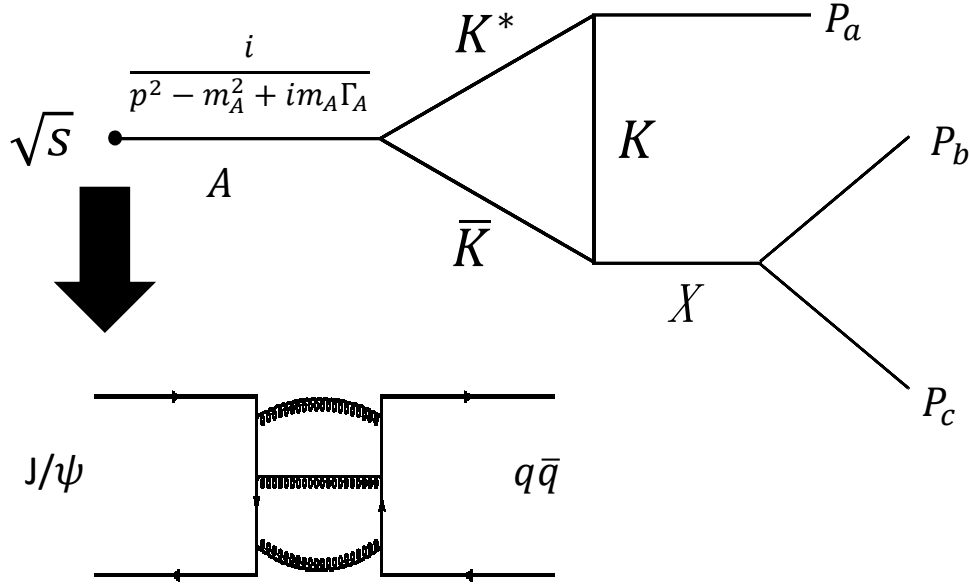


Fig. 5 A typical triangle diagram calculated, where the “A” stands for the light axial vector mesons, and X is some intermediate state (ρ, a_0, f_0 , etc.).

Typical production processes:

$$J/\psi \rightarrow \gamma f_1, \omega f_1, \phi f_1, \rho f_1$$

$$J/\psi \rightarrow \gamma a_1, \rho a_1, \omega a_1, \phi a_1$$

$$J/\psi \rightarrow \eta h_1, \eta' h_1, \pi h_1$$

$$J/\psi \rightarrow \pi b_1, \eta b_1, \eta' b_1$$

The production vertex can be estimated with the definition of mixing above, we have

For h_1 states

$$\begin{cases} h_1 = \cos(\alpha_{1P_1}) h_n + \sin(\alpha_{1P_1}) h_s \\ h'_1 = \cos(\alpha_{1P_1}) h_s - \sin(\alpha_{1P_1}) h_n \end{cases}$$

If then we assume $\langle i|H|s\bar{s} \rangle = \langle i|H|q\bar{q} \rangle = g_0$

The production amplitude can be simplified to

$$M_{i \rightarrow h_1} = g_0 (\sqrt{2} \cos(\alpha_{1P_1}) + \sin(\alpha_{1P_1}))$$

and

$$M_{i \rightarrow h'_1} = g_0 (\cos(\alpha_{1P_1}) - \sqrt{2} \sin(\alpha_{1P_1}))$$

Results of h_1, h'_1

Constraints:

1. $f_1(1420) \rightarrow \phi\gamma$ is not seen means $\alpha_{3P_1} \rightarrow 0^\circ$, which means $\alpha_{1P_1} \approx 20^\circ$. (Ref: Hai-Yang Cheng, PLB770, 116 (2012))
2. $\Gamma_{h_1} = 360 \pm 20\text{MeV}$ and fitting with the line-shape of $h_1 \rightarrow \rho\pi \rightarrow \pi^+\pi^-\pi^0$
3. In this case the contribution of TSM is different from that in f_1 and a_1 decay.

Estimation of production rate:

$$\begin{cases} \langle i|h_1 \rangle = \cos(\alpha_{1P_1}) \langle i|h_n \rangle + \sin(\alpha_{1P_1}) \langle i|h_s \rangle \\ \langle i|h'_1 \rangle = -\sin(\alpha_{1P_1}) \langle i|h_n \rangle + \cos(\alpha_{1P_1}) \langle i|h_s \rangle \\ \langle i|s\bar{s} \rangle = \langle i|q\bar{q} \rangle \end{cases}$$

Then the relative production rate(r.p.r.) is:

$$r.p.r. \equiv \frac{\langle i|h'_1 \rangle}{\langle i|h_1 \rangle} = \frac{-\sqrt{2}\sin(\alpha_{1P_1}) \langle i|h_n \rangle + \cos(\alpha_{1P_1}) \langle i|h_s \rangle}{\sqrt{2} \cos(\alpha_{1P_1}) \langle i|h_n \rangle + \sin(\alpha_{1P_1}) \langle i|h_s \rangle}$$

We found for $g_{h_1\rho^0\pi^0} = 4.32\text{GeV}$

$$\Gamma_{h_1} = 375\text{MeV}$$

$$\left. \begin{aligned} \Gamma_{h'_1 \rightarrow \rho\pi \rightarrow \pi^+\pi^-\pi^0} &= 79\text{MeV} \\ \Gamma_{h'_1 \rightarrow K\bar{K}\pi} &= 43\text{MeV} \end{aligned} \right\} \Gamma_{h'_1} = 122\text{MeV}$$

(PDG: 80~170MeV)

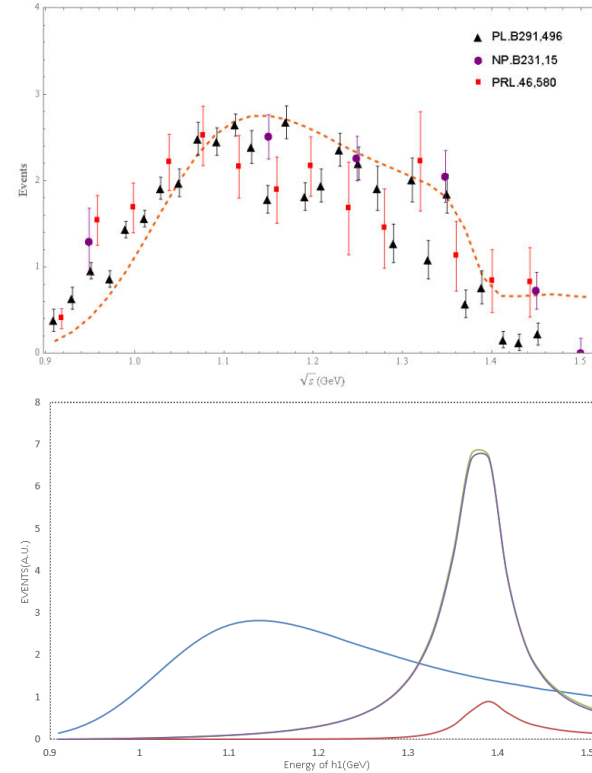
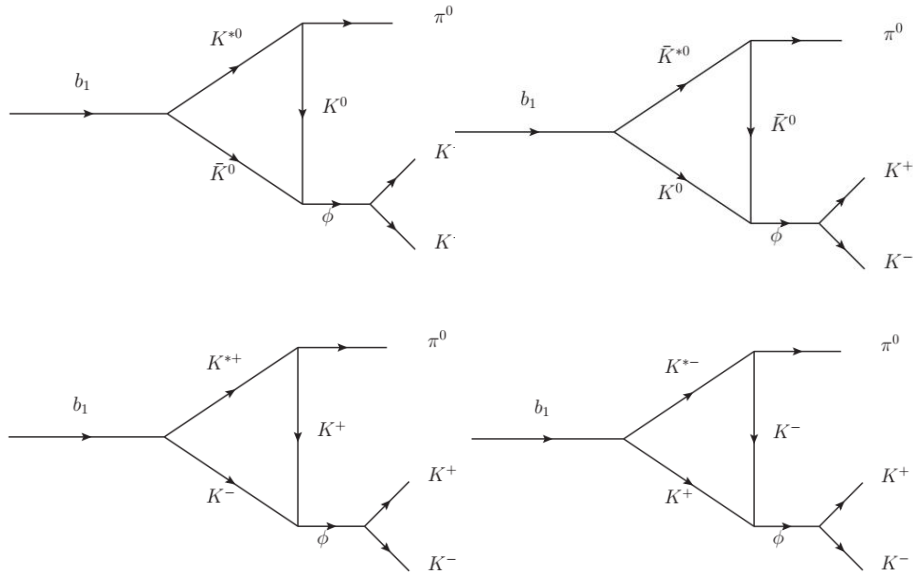


Fig. 6. The spectrum of $h_1 \rightarrow \rho\pi \rightarrow \pi^+\pi^-\pi^0$ compared with experiments, the contribution from triangle diagram of $h_1(1380)$ is shown in red in the lower figure.

Data: PL, B291, 496; PRL, 46, 580; NP, B231, 15

Results of b_1

From SU(3) symmetry, $b_1 \rightarrow \phi\pi \rightarrow K\bar{K}\pi$ is calculated. This process is OZI suppressed so that the leading order contribution is from triangle diagram.



$$\Gamma_{b_1 \rightarrow \phi\pi \rightarrow K\bar{K}\pi} = 0.46 \text{ MeV}$$

$$BR(b_1 \rightarrow \phi\pi \rightarrow K\bar{K}\pi) = 3.67 \times 10^{-3} \text{ (PDG: } < 4 \times 10^{-3} \text{)}$$

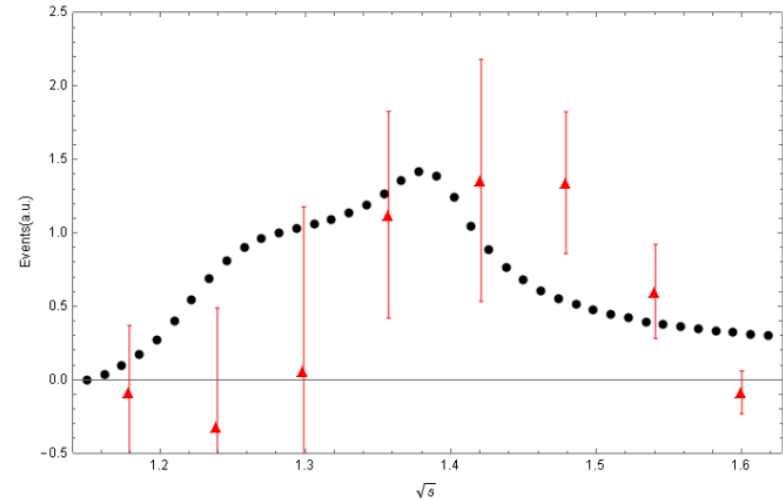


Fig. 7. Spectrum of $b_1 \rightarrow \phi\pi \rightarrow K\bar{K}\pi$. An apparent structure at 1.39 GeV is generated from triangle singularity, whereas the $b_1(1235)$ is absent, although the propagator of $b_1(1235)$ has been included to plot the spectrum (**black dot**).

Data: PAN, 59, 1184 (1996)

This is just a comparison with data obtained by $\pi^- p \rightarrow b_1^-(1235) n \rightarrow \phi\pi$. In this case the mixing angle dependence in production is not a good approximation. However, the data also implies a structure been at 1.4 GeV.

Results of f_1

1. With the help of Gell-Mann-Okubo relation $m_{f_1'(\alpha_{3P_1})} \sim 1.42\text{GeV}$, when $\alpha_{3P_1} = 10^\circ$. $f_1(1510)$ is excluded as the $q\bar{q}$ partner of $f_1(1285)$.
2. $BR(a_1(1260) \rightarrow \rho^\pm \pi^\mp (S\text{-wave})) = 60\%$ and $BR(f_1(1285) \rightarrow \pi^+ \pi^- \pi^0) = 3.0 \pm 0.9 \times 10^{-3}$ are used to estimate the coupling $g_{f_1 K^* \bar{K}}$ and the relative phase arising from $g_{f_0 K \bar{K}}$ between diagrams in Fig.5.

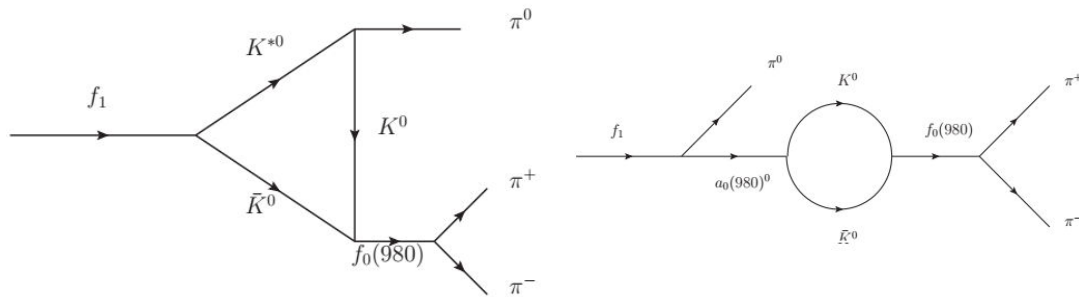


Fig. 8 The $a_0 - f_0$ mixing as well as the triangle is considered in $f_1(1285) \rightarrow f_0 \pi \rightarrow \pi^+ \pi^- \pi^0$

For $f_1(1285) \rightarrow a_0 \pi \rightarrow \eta \pi \pi$ and $f_1(1285) \rightarrow K^* \bar{K} \rightarrow K \bar{K} \pi$, it is the coupling $g_{f_1 a_0 \pi}$ and the relative phase from $a_0 K \bar{K}$ vertex are to be determined from partial width of $\eta \pi \pi$.

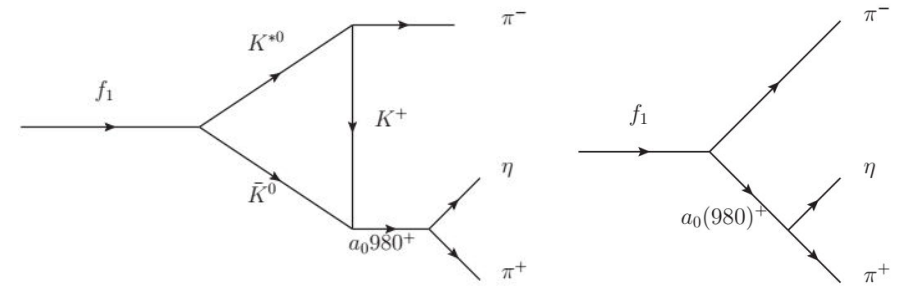


Fig. 9 Sample diagrams for $f_1(1285) \rightarrow a_0 \pi \rightarrow \eta \pi^+ \pi^-$

Result:

1. $BR(f_1(1285) \rightarrow \pi^+ \pi^- \pi^0) = 3.3 \times 10^{-3}$ (PDG: $3.0 \pm 0.9 \times 10^{-3}$)
2. $BR(f_1(1285) \rightarrow a_0 \pi \rightarrow \eta \pi \pi) = 35.9\%$ (PDG: $38 \pm 4\%$)
3. $BR(f_1(1285) \rightarrow K \bar{K} \pi) = 8.7\%$ ($9 \pm 0.4\%$)

Results of f_1

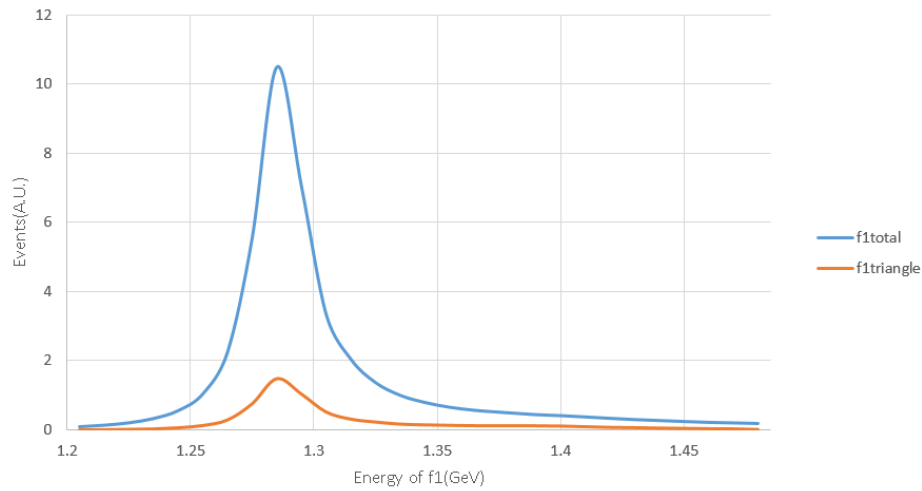


Fig. 10 Spectrum of $f_1(1285) \rightarrow \eta\pi\pi$ (blue), where the contribution from triangle diagrams are plotted in red.

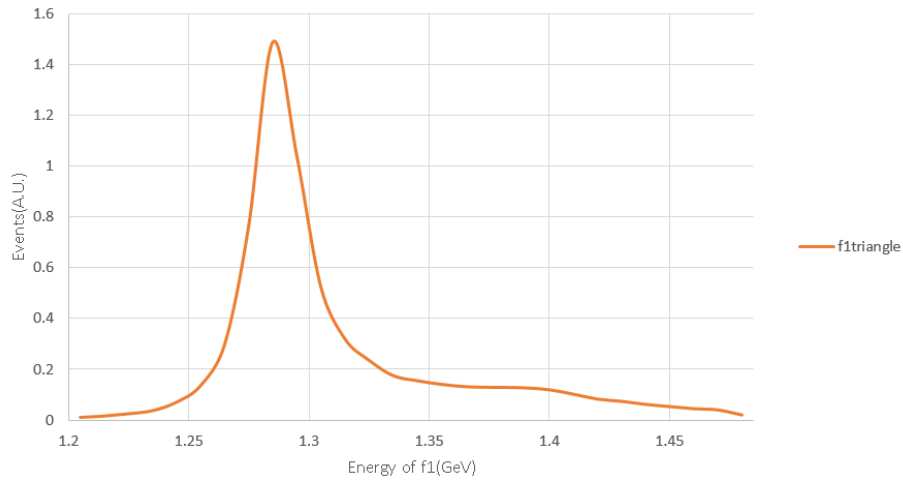
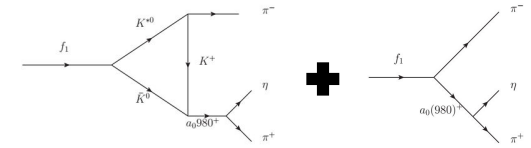
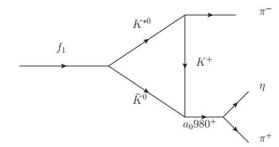
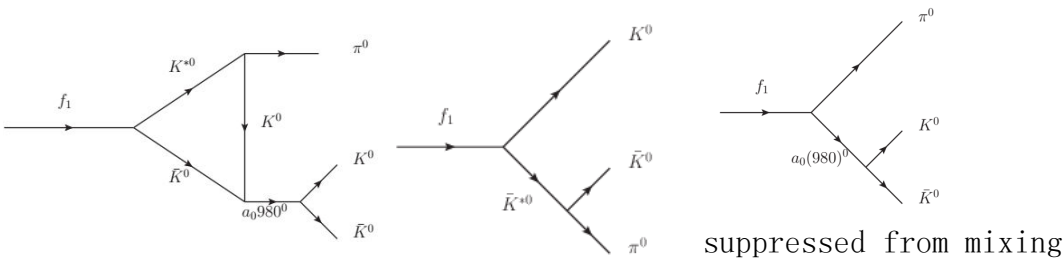


Fig. 11 Spectrum of $f_1(1285) \rightarrow \eta\pi\pi$ via triangle only (the red line in Fig. 7). A small shoulder can be seen if the tree diagram $f_1(1285) \rightarrow a_0\pi \rightarrow \eta\pi\pi$ is omitted.



Results of f_1'

The parameters are consistent with the fact that $f_1(1420)$ is absent in $a_0(980)\pi$ channel, even though the following decay modes for $f_1(1420)$ are considered:



The line shape of $K\bar{K}$ spectrum shows no $a_0(980)$ enhancement above $K\bar{K}$ threshold:

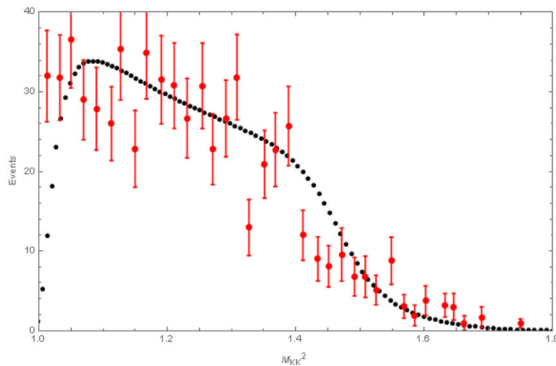


Fig. 12 $K\bar{K}$ spectrum of $f_1 \rightarrow a_0\pi(K^*\bar{K}) \rightarrow K\bar{K}\pi$

Data: T. A. Armstrong, et al. PL, B221, 216 (1989)

We estimated the $\eta\pi\pi$ spectrum (yellow line) for J/ψ radiative decay where the interference between $f_1(1285)$ and $f_1(1420)$ has been considered. (Note that no significant $f_1(1420)$ signal has been seen in pp scattering.

Ref: PL, B440, 225; PRL, 57, 1296)

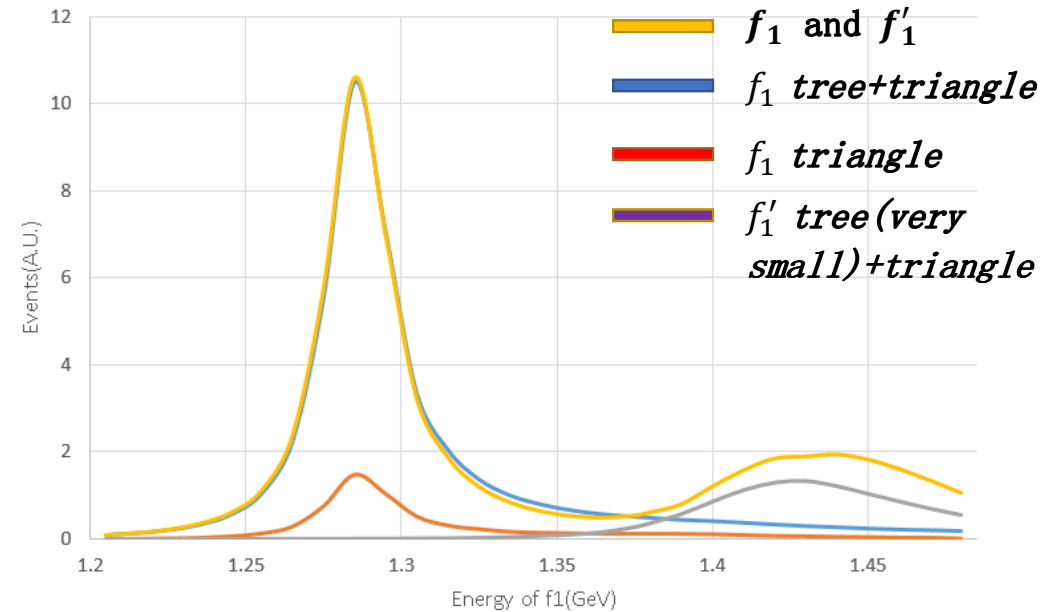


Fig. 13 $\eta\pi\pi$ spectrum of $f_1, f_1' \rightarrow \eta\pi\pi$.

Exp:

$$\frac{\Gamma_{\eta\pi\pi}}{\Gamma_{K\bar{K}\pi}} < 10\%$$

$$\frac{\Gamma_{\eta\pi\pi}}{\Gamma_{K\bar{K}\pi}} = 41\%$$

Comments on $f_1(1420)$:

1. The structure of $f_1(1420)$ in total f_1 spectrum (Yellow line) above comes by assuming $f_1(1420)$ as a genuine $q\bar{q}$ state.
2. This assumption is reasonable because otherwise it's hard to understand a significant pole at 1.4GeV is seen in $K\bar{K}\pi$ spectrum.
3. The intensity of $f_1(1420)$ is small compared to that of $f_1(1285)$, this is because when $f_1(1420)$ is taken as the partner of $f_1(1285)$, the small mixing angle makes the tree level $f_1(1420) \rightarrow \eta\pi\pi$ negligible, and the leading order contribution is from triangle diagram, whereas the tree diagram $f_1(1285) \rightarrow \eta\pi\pi$ is dominant for $f_1(1285)$ in $\eta\pi\pi$ channel.

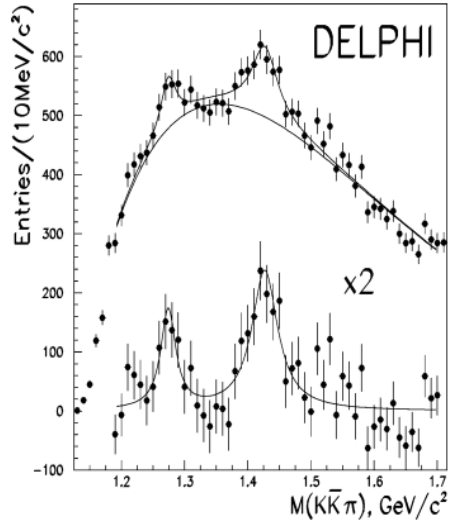


Fig. 14 The $K_s^0 K^\pm \pi^\mp$ invariant mass spectrum of $Z \rightarrow (K_s^0 K^\pm \pi^\mp) + X^0$. The solid curve is the fit with two simple Breit-Wigner. The pole of $f_1(1420)$ in this channel is very significant.

Data: J. Abdallah, etc PLB569, 129 (2003)

With the parameters so far obtained, the 3-body invariant mass spectrum for I breaking $a_1(1260) \rightarrow \eta\pi^0\pi^0$ is given with a constant width $\Gamma_{a_1(1260)total} = 280MeV$ calculated.

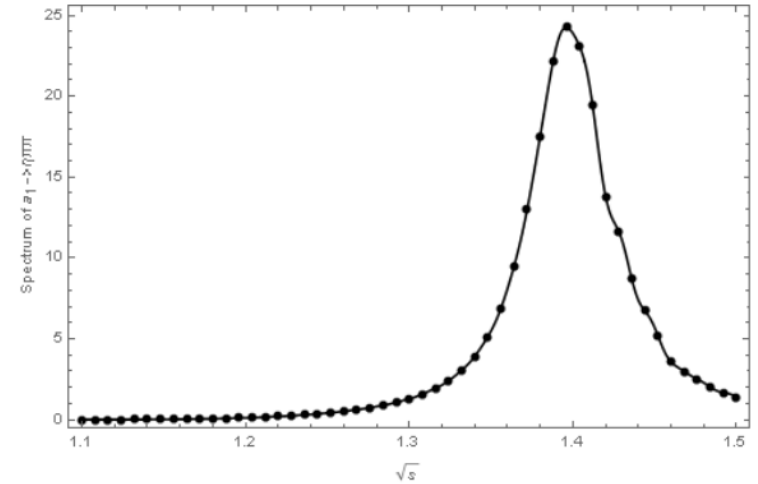


Fig. 15 3-body spectrum of $a_1^0(1260) \rightarrow \eta\pi^0\pi^0$. A much narrower structure at 1.4GeV is evident ($\Gamma \sim 50MeV$). It is narrow because when the condition of triangle singularity is fulfilled, the width of the pole from TS is mainly determined by the width of particles on the triangle. (In our case, it's $K^*K\bar{K}$)

Conclusions

- There are indeed some observable effects on the line shape of light axial vector invariant mass spectrum from the triangle singularity mechanism.
- The TSM does not have much impact on the spectrum of $h_1 \rightarrow \pi^+\pi^-\pi^0$, and the mixing angle $\alpha_{1\rho_1}$ is determined based on the mass relation as well as some experimental results.
- $b_1(1235) \rightarrow \phi\pi$ is a direct manifestation of triangle mechanism, with the predicted branching ratio being 3.67×10^{-3} just below the upper limit by experiment. The line shape is modulated by the propagator and the triangle mechanism.
- In isospin violated process $f_1(1285) \rightarrow \pi^+\pi^-\pi^0$, the impact of triangle diagrams is critical, which makes the total width 14% smaller than that with only $a_0 - f_0$ mixing amplitude.
- The triangle diagram could generate a shoulder at 1.4GeV in $f_1(1285) \rightarrow \eta\pi\pi$, but this structure is barely seen when the dominant tree level diagram $f_1(1285) \rightarrow a_0\pi \rightarrow \eta\pi\pi$ is taken into account.
- $a_1(1260) \rightarrow \eta\pi\pi$ also shows the effect of TSM by a much narrower resonance like structure at 1.4GeV.
- It's reasonable to assume $f_1(1420)$ being the isospin partner of $f_1(1285)$ from calculation of the mass of f_1' . Its production in J/ψ radiative decay is suppressed due to the mixing. Without the pole of $f_1(1420)$ it is hard to understand its signal in $KK\text{-bar}\pi$ and $\eta\pi\pi$ channels.

THANK YOU